

# ХИМИЧЕСКИЕ НАУКИ

## STUDY THE EFFECT OF (HF / H<sub>2</sub>O<sub>2</sub>) CONCENTRATION ON POROUS SILICON NANOWIRES BIOAPPLICATIONS BY AG-ASSISTED ELECTROLESS ETCHING METHOD

Muhannad M. Qassime<sup>1,2</sup>, D.O. Kochnev<sup>1</sup>, Denis V. Terin<sup>1</sup>, Sergey B. Venig<sup>1</sup>

<sup>1</sup>Department of Nano- and Biomedical Technologies, Saratov State University, Saratov, 410012, Russia

<sup>2</sup>Ministry of Science and Technology, Department of Chemical and Pharmaceutical Analysis, Baghdad, Iraq

e-mail: [muhannadmq77@gmail.com](mailto:muhannadmq77@gmail.com)

### Abstract:

We report on the structural and optical properties of porous silicon nanowires (PSiNWs) fabricated using silver (Ag<sup>+</sup>) ions assisted electroless etching method we prepare vertical and single crystalline PSiNWs via a two-step metal-assisted electroless etching method. The porosity of the nanowires is restricted by etchant concentration, etching time and doping level of the silicon wafer. The diffusion of Ag<sup>+</sup> ions could lead to the nucleation of silver nanoparticles on the nanowires and open new etching ways. Like porous silicon (PS), these PSiNWs also show excellent photoluminescence (PL) properties. The PL intensity increases with porosity, with an enhancement of about 100 times observed in our condition experiments. A “red-shift” of the PL peak is also found. These PSiNWs fabricated using the electroless etching method can find useful applications in biomedical and optical sensors.

**Keywords:** Porous silicon nanowires, Electroless etching, Silver catalyst, Porosity Photoluminescence,

### Introduction

The development of safe biomaterials is one of the most important aspects of modern biotechnology. Silicon (Si) has such properties as biocompatibility and bioavailability that allow it to be used to solve many biological and medical problems in the field of diagnosis and treatment of diseases, implantology and biomolecular imaging. [1-2]. Specific efforts have been concentrated in the development of new silicon nanostructures, including quantum dots, nanowires, or porous silicon (PS). PS is an excellent biomaterial taking into account its biocompatibility, biodegradability and bioresorbability [3,4]. In addition, the PS has also been combined with other biomolecules or materials introduced into its pores or deposited on its surface to produce composites [5] that can expand or develop their applications and properties [6-13]. PS has attracted much attention, especially in enhancing photo-emission. Much research efforts have been invested to realize an optical device with PS [14-16] but the inefficiency [17] and instability [18] of optical characteristic in PS still remain. In addition, porous silicon nanowires (PSiNWs) are also ideal candidate for the study of biophysics of low dimensional systems. It has potential impact in realizing nanoscale interconnects and functional device elements in future nanoscale electronic and optoelectronic devices [19,20]. Few attempts were focused on the luminescence of PSiNWs. Recently, it is found that this method can be used to synthesize a new silicon nanostructure named PSiNWs. The field of PSiNWs synthesis represents an exciting and rapidly expanding research area. Considerable efforts have been devoted to the development of versatile and controllable methods for the synthesis of PSiNW [21,22]. These methods can be broadly classified as: (i) bottom-up, and (ii) top-down approaches. The bottom-up approach involves the construction of desirable nanostructures from the basic components, i.e., from the atomic level to the nano- or micro-scale wires. This

method is useful for the fabrication of low-dimensional hetero structure based devices in large quantities. Using bottom-up, PSiNWs were first obtained by vapor-liquid-solid (VLS) method, followed by an etching step to create nanowires. The VLS method has been implemented in a variety of techniques, such as pulsed laser deposition (PLD) gas-phase molecular beam epitaxy (GS-MBE) chemical vapor deposition (CVD) laser ablation and oxide assisted growth techniques. Top-down approach seeks to fabricate PSiNWs from high quality single crystal silicon wafer or thin film. Silicon nanowires have also been realized using lithographically defined patterns, or spin-coating of nano-spheres as etched mask followed by etching of the nanowires using plasma processing technique. The fabrication of silicon nanowires using the metal-assisted electroless etching method has also been adopted [23-25]. Silver (Ag<sup>+</sup>) ions in an ionic solution of hydrofluoric acid (HF) and hydrogen peroxide (H<sub>2</sub>O<sub>2</sub>) have been used to the arrays of PSiNWs from single crystal wafers. The effects of various process parameters such as the etchant concentration of H<sub>2</sub>O<sub>2</sub>, etching time and post-etches treatment on the morphology and optical properties of the PSiNWs have also been investigated. Furthermore, this technique is effective, having high throughput and low cost [26-28]. In this work: We synthesized PSiNWs with different parameters, including the etchant concentration, etching time. The variable morphology of the PSiNWs is present, and the etching mechanism is discussed. The photoluminescence (PL) properties dependent on the processing parameters are also investigated here.

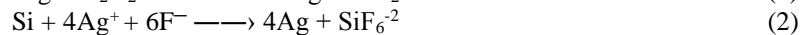
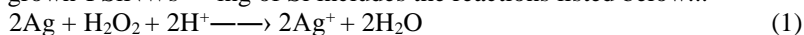
### Experiments

PSiNWs arrays were prepared by Ag-assisted electroless etching of 0,03 Ω×cm (100) p-type boron doped and 0,01 Ω×cm (111) n-type phosphorus doped mono-crystalline silicon wafers. The samples were firstly washed with acetone and deionized water and then immersed into a piranha solution H<sub>2</sub>SO<sub>4</sub> / H<sub>2</sub>O<sub>2</sub> in

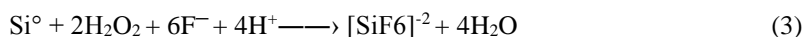
a volume ratio of 3:1 to remove the organic contaminants on the surface for 20 min. The thin oxide layer formed on the surface was then dissolved in a 5% HF solution. This treated wafer was transferred into an Ag deposition solution containing 4.8 M HF and 0.005 M AgNO<sub>3</sub> for 1 min at room temperature. The Ag nanoparticles (AgNPs) coated samples were sufficiently rinsed with deionized water to remove extra silver ions and then soaked into an etchant bath. The HF concentration of the etching solutions in the first group was fixed 5 M, while the H<sub>2</sub>O<sub>2</sub> concentrations vary 0.1, 0.2, 0.3, 0.4 and 0.5 M. The etching times are 30, 60, 90, 120 and 180 min. Samples were rinsed again for 10 min with HNO<sub>3</sub> solution to dissolve the excessive AgNPs, leaving behind traces of Ag for catalysing the etching reaction. The surface morphology of PSiNWs arrays were characterized by scanning electron microscopy SEM Tescan MIRA II LMU. The photoluminescence (PL) measured were performed at room temperature using Photoluminescence peaks were obtained on confocal Raman microscope Renishaw system.

### Results and Discussions

In the presence of Ag catalyst, an increase in HF or H<sub>2</sub>O<sub>2</sub> concentration in electroless etching method is analogous to an increase in the current density in electrochemical based methods [29,31]. In both cases, increasing the H<sub>2</sub>O<sub>2</sub> or HF concentration increases the oxidation rate and dissolution rate, respectively, resulting in nanostructures with varying optical properties [31]. From SEM images of the as-grown PSiNWs



The total reaction....

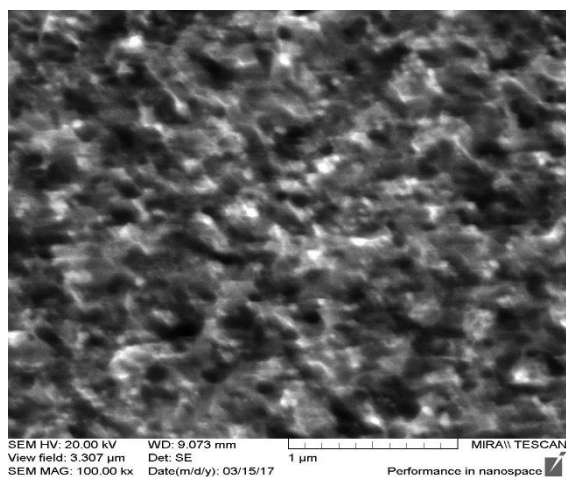


From Eq. 3, the potential for the etching process could be expressed as below.

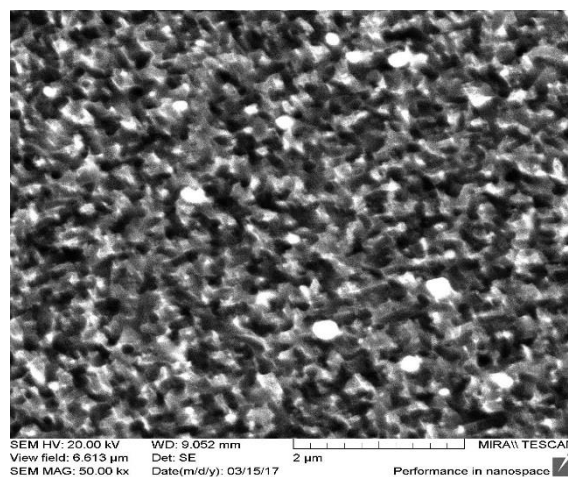
$$\Delta E = \Delta E^\circ - (0.056/4) \log \left( \frac{[\text{SiF}_6]^{2-}}{[\text{H}_2\text{O}_2]^2 [\text{H}^+]^4 [\text{F}^-]^6} \right) \quad (4)$$

etched with different H<sub>2</sub>O<sub>2</sub> concentrations and fixed HF concentration figure 1, the nanowires distribute uniformly on the whole wafers and are vertical to the substrate surface. The nanowires etched with lower H<sub>2</sub>O<sub>2</sub> concentrations are isolated from each other. However, when the concentration of H<sub>2</sub>O<sub>2</sub> increases, the tips of the nanowires congregate together. The diameters of the congregated bundles are several micrometres from the top view. These congregated bundles are also uniformly distributed on the entire wafers and could be confirmed from the cross-section images. Also, It's found that the surface of the nanowires becomes rough and the porosity (or the density) of the nanoporous increases with H<sub>2</sub>O<sub>2</sub> concentration. From our condition experiments, we found that the nanoporous appear from the lowest H<sub>2</sub>O<sub>2</sub> concentration of 0.1 M, for which the pores are smaller (several nanometres) and porosity is rather low.

This is different from the earlier report [32] which pointed out that the nanoporous did not appear, but only rough surface was found until the H<sub>2</sub>O<sub>2</sub> concentration was high enough. With the increase of H<sub>2</sub>O<sub>2</sub> concentrations, the pores also seem to grow, with the diameters ranging from several nanometres to nearly 10 nm for higher H<sub>2</sub>O<sub>2</sub> concentrations. The earlier report which pointed out that H<sub>2</sub>O<sub>2</sub> concentration is the key factor of the porosity varieties, while the etching time could only increase the thickness of the porous layer. The length variation of the nanowires with H<sub>2</sub>O<sub>2</sub> concentration is shown in figure 2. The chemical etching of Si includes the reactions listed below...



(a)



(b)

Figure 1: SEM images of the variable morphology of PSiNWs etched with: a) 0.1 M H<sub>2</sub>O<sub>2</sub>/5MHF b) 0.5 M H<sub>2</sub>O<sub>2</sub>/5MHF.

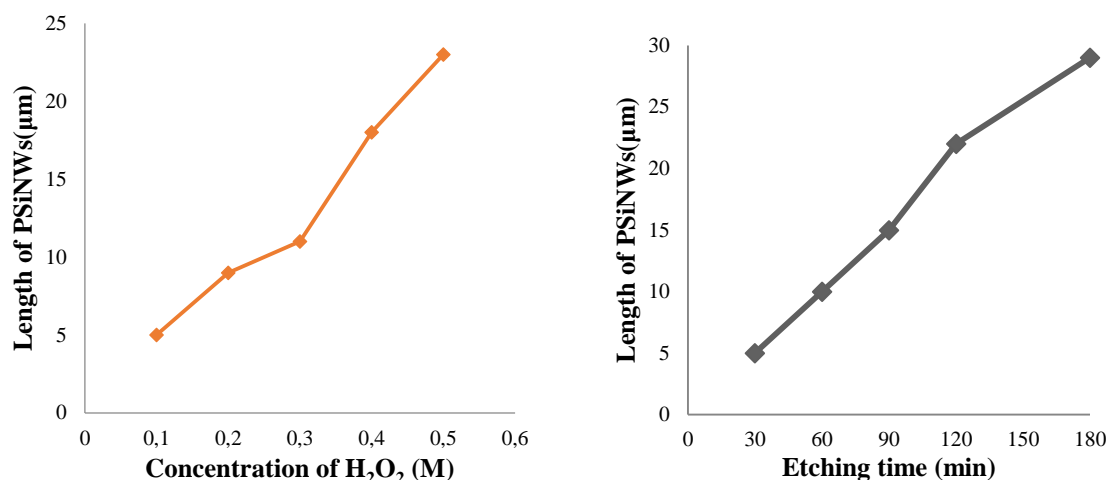


Figure 2: The length of PSiNWs depends on H<sub>2</sub>O<sub>2</sub> conc. and etching times.

The increase in H<sub>2</sub>O<sub>2</sub> concentration could enhance the potential for the etching process, which indicates that the etching reaction is more thermodynamically favoured and the etching could be accelerated. Therefore, the length of the nanowires is not only time dependent, but also relies on the oxidant concentration. As the catalyst, the AgNPs are oxidized into Ag<sup>+</sup> ions by H<sub>2</sub>O<sub>2</sub>. The Ag<sup>+</sup> ions extract electrons from Si nearby and are deoxidized into Ag again.

The Si atoms around are oxidized and dissolved, leading to the etching of the silicon surface and the formation of the vertical PSiNW arrays. However, during the etching process, the Ag<sup>+</sup> ions could not be recovered to Ag totally. Ag<sup>+</sup> ions with certain concentration around the AgNPs would diffuse out to the tips of the PSiNWs, where the concentration of Ag<sup>+</sup> ions is lower. For the lightly doped silicon wafer, the Ag<sup>+</sup> ions along with the PSiNWs are difficult to be deoxidized into smaller AgNPs as the lack of defective sites for new nucleation. So the diffused Ag<sup>+</sup> cannot etch the side-walls of the PSiNWs and no porous structure appears. However, for the heavily doped silicon wafers, the dopants could induce amount of weak defective points in the silicon lattices. These defective points could serve as the nucleation centres. When the Ag<sup>+</sup> ions near the defective points reach a critical concentration, the Ag<sup>+</sup> will nucleate on the side walls or the tips of the PSiNWs and the smaller AgNPs appear. These newly formed AgNPs open new etching pathways on the PSiNWs and facilitate the formation of the nanopores. Furthermore, the nucleation of the AgNPs on the side walls would also reduce the Ag<sup>+</sup> concentration and accelerates the Ag<sup>+</sup> diffusion. When the Ag<sup>+</sup> ions concentration reaches the critical value again, new nucleation occurs. This could be confirmed by our results

listed in figure 2, the porosity of the nanowires increases with the etching time, which indicates that new AgNPs appear and new nanopores form with time. It could also be found that some nanopores overlap on the side walls, especially for the PSiNWs etched with longer time. It is because new AgNPs nucleation takes place near the defects distributed on the wires, some nucleation centres stay near the formed nanopores, and the newly etched pores would overlap with the original ones. It could also explain why the nanopores seem to grow larger with times. From this mechanism, we could deduce that the side walls on the topside of the wires have higher porosity compared with the down-side. As the nanowires were scraped from the wafers, the cuts of the wires are trim. However, the tips are fragmentary as shown in the SEM image. It could be clearly seen that the porosity increases and the nanopores grow larger from the bottom to the top tip. The increase in H<sub>2</sub>O<sub>2</sub> concentrations could accelerate the oxidation of Ag and increase the Ag<sup>+</sup> ions concentrations, leading to more additional etching pathways and higher porosity. It could be concluded that the doping level of the silicon wafer, the H<sub>2</sub>O<sub>2</sub> concentration and the etching time are the key factors for the nanoporous formation on the PSiNWs.

The room temperature PL measurement was carried out to study the optical properties of the PSiNWs with different H<sub>2</sub>O<sub>2</sub> concentrations figure 3, display the PL spectrums of the PSiNWs. The increase in the H<sub>2</sub>O<sub>2</sub> concentration, the porosity of the nanowires increases and leads to the PL intensity enhancement. The PL intensity of PSiNWs etched with 0.5 M H<sub>2</sub>O<sub>2</sub> is almost more high as the samples etched with 0.1 M H<sub>2</sub>O<sub>2</sub>. When the sample was etched for 3 h, an increase in the PL intensity by a factor of 40 is observed, compared with the 30 min-etched sample.

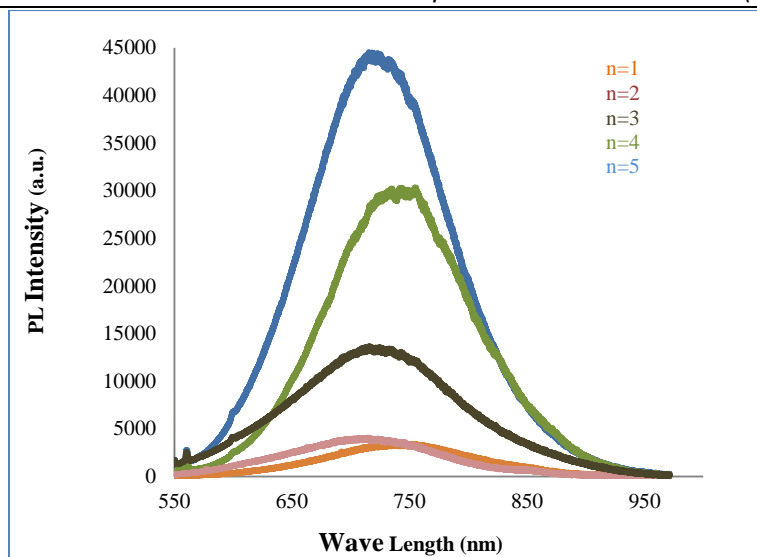


Figure3: The PL spectrums of the SiNWs correspond to the PSiNWs etched for 60 min with the  $H_2O_2$  concentrations of 0.1, 0.2, 0.3, 0.4 and 0.5 M, respectively.

However, it is unexpected to find that PL peaks of the samples with higher porosity seem to “red-shift” and are not well symmetrical. It is thought that higher porosity would decrease the size of the silicon nanostructure, which could lead to the blue-shift of the PL peak due to the quantum confinement effect. We also measure the PL spectrums of the samples treated with  $HNO_3$  but without HF solution, which are considered to have an oxide layer on the surfaces. It is found that the PL peaks are fixed at  $\sim 730$  nm for all the samples. The PL intensity varieties with the preparation parameters are similar with the samples with HF treatment.

### Conclusion

In summary, we carried out chemical etching on the highly doped p-type and n-type silicon (100) wafers to synthesize the PSiNW arrays. We found that longer etching time or higher  $H_2O_2$  concentration could facilitate the diffusion and nucleation of  $Ag^+$  ions and effectively enhance the porosity of the nanowires. The PL intensity could be effectively enhanced by the increased porosity. The emission intensity from the local porous structure quickly enhances with the porosity and takes up the leading place of the PL spectrum, resulting in the “red-shift” observed. These PSiNWs combine the physical properties of PSiNWs and PS and could lead to opportunities for new generation of nanoscale optoelectronic devices can be potentially useful in optical sensors applications.

### References

1. Sripanyakorn S., Jugdaohsingh R., Nutrition Bull. 30 (2005) 222.
2. Parkilla T., Hakala M., Kautiainen H., Leppilahti J., Belt E.A., Scand.J Plast.Reconstr. Surg. 40, (2006) 297-301.
3. Chan CK, Peng HL, Liu G, McIlwrath K, Zhang XF, Huggins RA, Cui Y: Nat. Nanotechnol. 3 (2008) 31.
4. Y. Qu, H. Zhou, and X. Duan ,Nanoscale3. 3(10) (2011) 4060.

5. Z. G. Bai, D. P. Yu, J. J. Wang, Y. H. Zou, W. Qian, J. S. Fu, S. Q. Feng, J. Xu, and L. P. You, Mater. Sci. Eng., B72 (2000)117.
6. Canham L.T. Biomedical MEMS: Clinical Applications of Silicon Technology, Inst. of Physics. 921 (2003).-7503.
7. J. Paczesny, A. Kamińska, W. Adamkiewicz, K.Winkler, K. Sozanski, M.Wadowska, I. Dziecielewski, R.Holyst , Chem. Mater. 24 (2012).3667
8. Lehman V. Electrochemistry of silicon: instrumentation, science, materials and applications. Wiley-VCH, Weinheim. (2002)286.
9. T.E. Goto, R.F. Lopez, O.N. Oliveira Jr., L. Caseli,Langmuir .26 (2010) 11135
10. A-M.S. Aurélie, C J. B. Loï, A.M. Christophe, P.G-E.Agnès, Langmuir. 26 (2009) 2160.
11. M.L. Hammock, O. Knopfmacher, B.D. Naab, J.B.H.Tok, Z. Bao, ACS Nano.7 (2013)3970.
12. D.F. Moyano, V.M. Rotello, Langmuir .27 (2011)10376.
13. T.E. Goto, R.F. Lopez, O.N. Oliveira Jr., L. Caseli,Langmuir. 26 11135(2010).
13. A-M.S. Aurélie, C J. B. Loï, A.M. Christophe , P.G-E.Agnès, Langmuir 26 (2009).2160.
14. A. Najar, J. Charrier, H. Ajlani, N. Lorrain, S. Haesaert, M. Oueslati, and L. Haji, Mater. Sci. Eng., 146B, 260 (2008).
15. A. Najar, N. Lorrain, H. Ajlani, J. Charrier, M. Oueslati, and L. Haji,Appl. Surf. Sci. 256 (2009) 581.
16. A. Najar, H. Ajlani, J. Charrier, N. Lorrain, S. Haesaert, M. Oueslati, and L. Haji, Physica B 396 (2007) 145.
17. H. Koyama, T. Nakagawa, T. Ozaki, and N. Koshida, Appl. Phys. Lett. 65 (1994) 1656.
18. L. T. Canham, M. R. Houlton, W. Y. Leong, C. Pickering, and J. M. Keen,J. Appl. Phys. 70 (1991) 422.
19. Y. Huang, X. Duan, and C. M. Lieber, Small 1, (2005) 142.
20. M. T. Bohr, IEEE Trans. Nanotechnol. 1, (2002) 56.

21. C. M. Lieber, Solid State Commun. 107, (1998) 607.
22. Y. N. Xia, P. D. Yang, Y. G. Sun, Y. Wu, N. Mayers, B. Gates, Y. Yin, F. Kim, and H. Yan, Adv. Mater. 15 (2003) 353.
23. A. I. Hochbaum, D. Gargas, Y. J. Hwang, and P. Yang, Nano Lett. 9, (2009) 3550.
24. D. Kumar, S. K. Srivastava, P. K. Singh, K. N. Sood, V. N. Singh, N. Dilawar, and M. Husain, J. Nanopart. Res. 12, (2010) 2267.
25. S. K. Srivastava, D. Kumar, P. K. Singh, M. Kar, V. Kumar, and M. Husain, Sol. Energy Mater. Sol. Cells 94(2010) 1506.
26. K. Q. Peng, Y. J. Yan, S. P. Gao, and J. Zhu, Adv. Mater. 14, (2002) 1164.
27. T. Qiu, X. L. Wu, Y. F. Mei, G. J. Wan, P. K. Chu, and G. G. Siu, J. Cryst. Growth. 277 (2005) 143.
28. X. Zhong, Y. Qu, Y. C. Lin, L. Liao, and X. Duan, ACS Appl. Mater. Interfaces. 3 (2011) 261–270.
29. E. S. Kooij, K. Butter, and J. J. Kelly, Electrochem. Solid State Lett. 2, (1999) 178.
30. D. R. Turner, J. Electrochem. Soc. 107 (1960) 810.
31. Y. Qu, H. Zhou, and X. Duan, Nanoscale 3 (2011) 4060.
32. Peng KQ, Wang X, Lee ST. Appl. 2009. p. 243112

УДК 539.12.04+621.314.2+621.315.61

## ИССЛЕДОВАНИЕ РАДИАЦИОННОЙ СТОЙКОСТИ ТРАНСФОРМАТОРНОГО МАСЛА В ПОЛЕ ИОНИЗИРУЮЩЕГО ИЗЛУЧЕНИЯ

*Искендерова З.И.,  
Курбанов М.А.*

*Институт Радиационных Проблем Национальной АН Азербайджана  
АЗ 1143, Баку, ул. Б.Вахабзаде, 9  
E-mail: [zenfira\\_iskenderova@mail.ru](mailto:zenfira_iskenderova@mail.ru)*

## STUDY ON RADIATION RESISTANCE OF TRANSFORMER OIL UNDER IONIZING IRRADIATION

*Iskenderova Z.I.,  
Gurbanov M.A.*

*Institute of Radiation Problems of National Science Academy of AR  
AZ 1143, Baku, Azerbaijan, B.Vakhabzadeh str. 9  
E-mail: [zenfira\\_iskenderova@mail.ru](mailto:zenfira_iskenderova@mail.ru)*

В данной работе исследованы изменения физико-химических параметров, как удельное сопротивление, вязкость, плотность и образование газообразных продуктов  $H_2$ ,  $CH_4$ ,  $C_2H_4$ ,  $C_2H_6$ ,  $C_3H_8$ ,  $C_4H_{10}$ ,  $C_5H_{12}$ ,  $C_6H_{14}$  в зависимости от поглощенной дозы в интервале (29,7–237,6) кГр. Установлено, что при воздействии  $\gamma$ -излучения на трансформаторное масло происходит изменения химического состава, что сопровождается изменением удельного сопротивления, вязкости и плотности масла. Степень превращения зависит от поглощенной дозы и растет с её ростом.

### ABSTRACT

Changes of physico-chemical parameters, as specific resistance, viscosity, density and formation of gaseous products as  $H_2$ ,  $CH_4$ ,  $C_2H_4$ ,  $C_2H_6$ ,  $C_3H_8$ ,  $C_4H_{10}$ ,  $C_5H_{12}$ ,  $C_6H_{14}$  on dependence of adsorbed doses was investigated. It was established, that the changes of chemical composition of oil leads to changes of specific resistance, viscosity, density. Degree of its conservation is increasing with adsorbed dose rising.

**Ключевые слова:** радиационная стойкость, трансформаторное масло,  $\gamma$ -излучения, радиационно-химические выходы, плотность, вязкость, удельное сопротивление

**Keywords:** radiation resistance, transformer oil,  $\gamma$  - radiation, radiation-chemical yields, density, viscosity, specific resistance

### ВВЕДЕНИЕ

Силовые трансформаторы широко используются в энергетическом секторе, в частности в атомной энергетике. В последнем случае возникает необходимость изучения радиационной стойкости трансформаторного масла.

Проблемы, связанные с радиационной стойкостью материалов электрических оборудования, возникающие в результате различных аварийных ситуации исследуются во многих работах, посвященных определению работоспособности различных узлов и агрегатов атомных электростанций [1]. Во-

просы особенно стало актуально после аварии Чернобыльской АЭС в 1986 год. После аварии Чернобыльской АЭС был идентифицирован ряд аварий с уровнем больше INES 4 (International Nuclear Events Scale) [2].

Находящиеся в Кавказском регионе Армянское АЭС периодически ремонтируются с целью устранения результатов аварийных ситуаций.

В работах [3, 4, 5] исследованы наиболее функционально значимые комплектующие материалы и электрооборудования - трансформаторное масло и электроизоляционный картон с целью определения возможного снижения надежности, в частности